Materials Chemistry and Physics 135 (2012) 193–205

Contents lists available at SciVerse ScienceDirect

Materials Chemistry and Physics

journal homepage: www.elsevier.com/locate/matchemphys

Understanding the reaction mechanism of *in-situ* synthesized (TiC–TiB_2)/AZ91 magnesium matrix composites

Mohammed Shamekh, Martin Pugh, Mamoun Medraj*

Department of Mechanical Engineering, Concordia University, 1455 de Maisonneuve Blvd. W., Montréal, Québec, Canada H3G 1M8

HIGHLIGHTS

- For the first time, MMC of Mg/(TiC_x–TiB_2 network) is fabricated without using Al.
- A practical and cost-effective *in-situ* reactive infiltration technique is developed.
- The effect of the infiltrated Mg on the reaction between Ti and B_4C is uncovered.
- The first attempt to study the effect of MgH_2 on the reaction mechanism.
- The formation of the Ti_2AlC ternary compound and its consequences are discussed.

ARTICLE INFO

Article history:
Received 10 December 2011
Received in revised form
5 April 2012
Accepted 29 April 2012

Keywords:
Composite materials
Electron microscopy
X-ray diffraction
Phase transitions

ABSTRACT

Magnesium matrix composites reinforced with a network of TiC and TiB_2 compounds have been successfully synthesized via an *in-situ* reactive infiltration technique. In this process, the ceramic reinforcing phases, TiC and TiB_2, were synthesized *in-situ* from the starting powders of Ti and B_4C without any addition of a third metal powder such as Al. The molten AZ91 magnesium alloy infiltrates the preform of 3Ti–B_4C by capillary forces. Furthermore, adding different weight percentages of MgH_2 powder to the 3Ti–B_4C preforms was used in an attempt to increase the Mg content in the fabricated composites. The results reveal a relatively uniform distribution of the reinforcing phases in the magnesium matrix with very small amounts of residual Ti, boron carbide and intermediate phases when they are fabricated at 900 °C for 1.5 h using a 3Ti–B_4C preform with 70% relative density. On the other hand, after adding MgH_2 to the 3Ti–B_4C preform, TiC_x and TiB_2 formed completely without any residual intermediate phases with the formation of the ternary compound (Ti_2AlC) at the expense of TiC. The percentage of reinforcing phases can be tailored by controlling the weight percentages of MgH_2 powder added to the 3Ti–B_4C preform. The results of the *in-situ* reaction mechanism investigation of the Ti–B_4C and Mg–B_4C systems show that the molten magnesium not only infiltrates through the 3Ti–B_4C preform and thus densifies the fabricated composite as a matrix metal, but also acts as an intermediary making the reaction possible at a lower temperature than that required for solid-state reaction between Ti and B_4C and accelerates the reaction rate. The investigation of the *in-situ* reaction mechanism with or without the addition of MgH_2 powder to the 3Ti–B_4C preforms reveals similar mechanisms. However, the presence of the MgH_2 in the preform accelerates the reaction resulting in a shorter processing time for the same temperatures.

1. Introduction

Magnesium matrix composites reinforced with suitable ceramic particles are attractive for different applications especially in automotive and aerospace industries due to their superior specific properties such as elastic modulus and strength, high wear resistance, and excellent thermal and electrical conductivities [1–3].

There are several methods to fabricate particulate reinforced Mg metal matrix composites (MMCs) by *ex-situ* routes including powder metallurgy, preform infiltration, spray deposition, mechanical alloying and different casting technologies such as squeeze casting, rheocasting and compocasting [4]. However, *in-situ* MMCs can exhibit excellent mechanical properties due to the formation of ultra-fine, homogeneously dispersed and thermodynamically stable ceramic reinforcements with clean reinforcement-

* Corresponding author.
E-mail address: mmedraj@encs.concordia.ca (M. Medraj).

0254-0584/$ – see front matter © 2012 Elsevier B.V. All rights reserved.
doi:10.1016/j.matchemphys.2012.04.054

matrix interfaces. Also, near-net-shape composites can be fabricated with a high volume percentage of the reinforcing ceramic phase at an effective cost [5, 6].

Different techniques such as self-propagating high temperature synthesis (SHS) and remelting and dilution have been used to fabricate Mg matrix composites reinforced with *in-situ* TiC and TiB_2 particles. For example, Ma et al. [7] using the SHS technique via a master alloy route starting with a low cost Al–Ti–B_4C system succeeded in fabricating TiB_2–TiC/Mg matrix composites. They are considered the first to use B_4C instead of B and/or C in the starting materials. On the other hand, Zhang et al. [8] successfully fabricated TiB_2–TiC/Mg matrix composites via the remelting and dilution technique using a preform of a sintered block of a mixture of Al–Ti–B_4C.

The main objective of this work is to synthesize Mg matrix composites reinforced with TiC and TiB_2 and to understand the *in-situ* reaction mechanism responsible for the formation of these compounds in the Mg matrix. Although *in-situ* reactive infiltration has been used before to fabricate Mg matrix composites reinforced with TiC particles starting from Ti and C powders [9], this is the first time such Mg matrix composites are synthesized starting from Ti and B_4C materials without adding Al using a practical and low cost technique.

2. Thermodynamic analysis

For understanding the *in-situ* reaction mechanism, reaction thermodynamics are used to calculate the reaction direction and the expected stable phases and their compositions at elevated temperatures. The potential reactions that can occur in the Mg–Ti–B_4C system and between the reactants and some intermediate phases are as follows:

$$\frac{2}{3}Mg + \frac{1}{3}B_4C = \frac{2}{3}MgB_2 + \frac{1}{3}C \quad (1)$$

$$\frac{1}{2}Ti + \frac{1}{2}C = \frac{1}{2}TiC \quad (2)$$

$$\frac{5}{6}Ti + \frac{1}{6}B_4C = \frac{2}{3}TiB + \frac{1}{6}TiC \quad (3)$$

$$\frac{16}{17}TiB + \frac{1}{17}B_4C = \frac{5}{17}Ti_3B_4 + \frac{1}{17}TiC \quad (4)$$

$$\frac{3}{4}Ti_3B_4 + \frac{1}{4}B_4C = 2TiB_2 + \frac{1}{4}TiC \quad (5)$$

$$\frac{2}{3}TiB + \frac{1}{3}MgB_2 = \frac{2}{3}TiB_2 + \frac{1}{3}Mg \quad (6)$$

$$\frac{1}{2}Ti + \frac{1}{2}MgB_2 = \frac{1}{2}TiB_2 + \frac{1}{2}Mg \quad (7)$$

$$\frac{2}{3}Ti + \frac{1}{3}MgB_4 = \frac{2}{3}TiB_2 + \frac{1}{3}Mg \quad (8)$$

$$\frac{3}{4}Ti + \frac{1}{4}B_4C = \frac{1}{2}TiB_2 + \frac{1}{4}TiC \quad (9)$$

To compare the feasibility and favorability of these reactions, the changes in the reaction enthalpy, ΔH, and the Gibbs free energy, ΔG, for one mole of the reactants were calculated as shown in Fig. 1. It can be observed from Fig. 1(a) that all reactions are exothermic (*−ve* ΔH) and have negative standard Gibbs free energy. Therefore, all reactions are thermodynamically feasible as shown in Fig. 1(b).

It is worth noting that ΔG_5 and ΔG_9 are more negative for the formation of TiC–TiB_2 in the temperature range of interest and thus reactions (5) and (9) have a higher tendency for the formation of TiC–TiB_2 than the other reactions. However, reaction (5) is considered as an intermediate reaction to form TiC–TiB_2. Therefore, from the thermodynamics point of view, it can be deduced that the final equilibrium phases should be TiB_2, TiC and Mg in the composite.

3. Experimental work

3.1. Fabrication of the composites

In this work, two systems of starting powders were used for synthesizing the TiC–TiB_2/Mg composites: System I, Ti–B_4C, consists of 72.2 wt.% Ti (−325 mesh, 99.61% purity, Alfa Aesar Co.) and 27.8 wt.% B_4C (99% purity, <10 μm particle size, Alfa Aesar Co.) powders. Titanium and boron carbide powders are at a molar ratio of 3:1 corresponding to that of stoichiometric TiC and TiB_2. System II, Ti–B_4C with MgH_2 powder, MgH_2 powder (98% purity, Alfa Aesar Co.) was added to the 3Ti–B_4C mixture at different weight percentages. The starting powders were mixed under Ar in a stainless steel jar with stainless steel balls inside a planetary ball mill, in which the ratio of the balls to the powder was 7:1 and the milling speed and time were 400 rpm and 5 h, respectively. In order to prevent oxidation, the mixtures were prepared in a glove box filled with Ar.

After full mechanical blending, the resulting mixture of Ti and B_4C powders was compacted at pressures ranging from 80 to 120 MPa into green compacts of cylindrical shape of 15 mm in diameter and variable heights with various relative densities of approximately 55, 60, 65, and 70% ± 2% using a hardened steel die with two plungers.

The *in-situ* reactive infiltration experiments were finally carried out in an electric furnace under the presence of flowing argon gas (purity ≥ 99.999%) as shown in Fig. 2(a). The heating cycle is shown in Fig. 2(b). The temperature was set in the range from 700 °C to 950 °C at 50 °C intervals, the holding time ranged from 1 to 6 h and the heating rate was 10 °C min^{-1}. The samples were naturally cooled down to room temperature.

3.2. Investigation of the reaction mechanism

3.2.1. Reaction mechanisms in the Mg–Ti–B_4C system

To understand the *in-situ* reaction mechanism for synthesizing TiC–TiB_2/AZ91D composites, the reaction mechanisms in the Ti–B_4C and Mg–B_4C systems have been investigated separately. For the Ti–B_4C system, 3Ti–B_4C green compacts with 70% relative density (*RD*) were heated to 900 °C and kept in the furnace at this temperature for different holding times (Δt) ranging from 1 to 10 h according to the heating cycle shown in Fig. 2(b). Also, to investigate the reaction sequence in the Ti–B_4C system experimentally, thin 3Ti–B_4C green compacts were prepared with 70% *RD* and placed in a quartz tube under Ar. The encapsulated samples were heat-treated at different temperatures from 600 to 900 °C for 1 h holding time and then quenched in water.

On the other hand, to investigate the effect of Mg melt during and after the spontaneous infiltration, two pure B_4C preforms were compacted at 70% *RD*. One of them was heated to 900 °C for 1 h and then naturally cooled down to room temperature while the other one was infiltrated by molten Mg at 900 °C for 1 h using the setup presented in Fig. 2(a). Also, the reaction sequence in the Mg–B_4C system was investigated in similar fashion to that of the Ti–B_4C

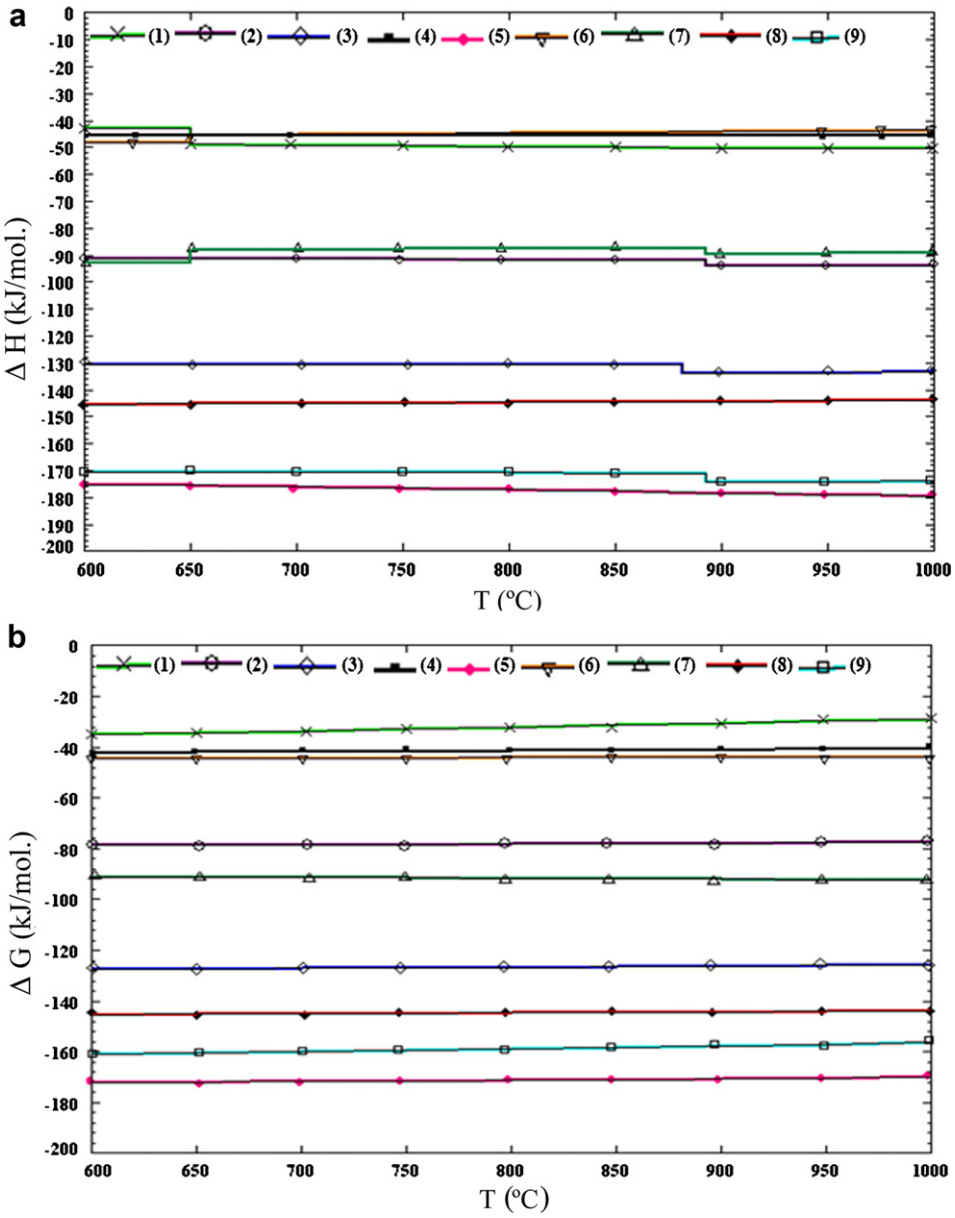

Fig. 1. Changes in (a) reaction enthalpy, Δ*H*, and (b) Gibbs free energy, Δ*G*, for reactions in the Mg–Ti–B_4C system. The numbers in brackets refer to the reaction numbers in Eq. (1)–(9).

system. The molar ratio of Mg to B_4C in these preforms is (2.7:1) which matches with 25 wt.% Mg powder in the preform and higher than that required to complete the reaction between Mg and B_4C to form MgB_2.

3.2.2. Reaction mechanism of the infiltrated Mg in the (MgH_2–Ti–B_4C) preform

To understand the *in-situ* reaction mechanism of the infiltrated Mg in the MgH_2–Ti–B_4C preform, the reaction mechanism was divided into four subsystems; MgH_2–Ti, MgH_2–B_4C, MgH_2–Ti–B_4C and Mg–Ti–B_4C. The latter was discussed in section 3.2.1. It is very important to note that the molar ratio of these individual system matches with 25 wt.% MgH_2 powder added to Ti and B_4C powders with 3:1 molar ratio.

The reaction sequence in the MgH_2–Ti system was investigated as that of Ti–B_4C system but the temperatures in this case were from 400 to 800 °C. Also, a (MgH_2–Ti) compact heat-treated at 900 °C for 1.5 h according to the heating cycle shown in Fig. 2(b) was compared with the composite sample fabricated using the same green compact after the infiltration of molten AZ91D at the same processing parameters. The same was performed for the MgH_2–B_4C system. The molar ratio of MgH_2 to B_4C in these compacts is (2.52:1) which matches with 25 wt.% MgH_2 powder in the preform.

Finally, 25 wt.% MgH_2–(3Ti–B_4C) compact at 70% *RD* heat-treated at 900 °C for 1.5 h was compared with an AZ91D matrix composite sample fabricated at the same temperature and holding time using a similar preform.

The microstructure and the phase analysis of the heat-treated preforms and the fabricated composite samples were investigated using scanning electron microscope (SEM) (Model, Philips XL30 FEG) equipped with Energy Dispersive X-ray spectroscopy (EDS) and XRD using an X-ray diffractometer, (X'Pert PRO, manufactured by PANalytical Inc.). It is important to note that Si is added to all

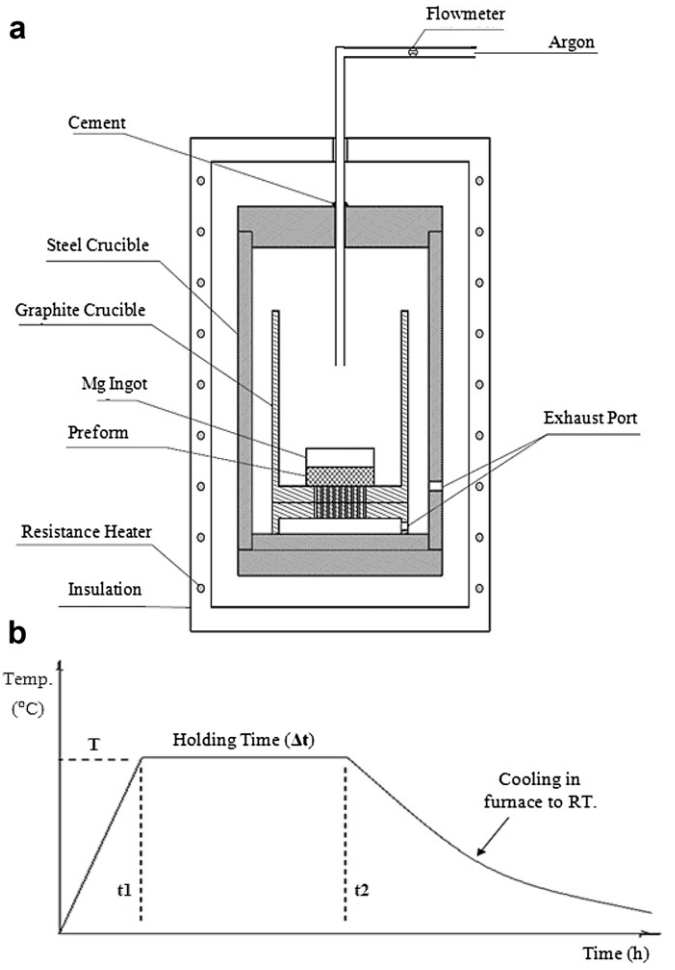

Fig. 2. Schematic experimental setup (a) and the heating cycle for the fabricating of the composite samples (b)

powder samples for XRD analysis as an internal standard to correct any systemic error.

4. Results and discussions

4.1. Fabrication of the (TiC–TiB_2)/AZ91D matrix composites

In this work, the influence of the processing temperature, holding time and the green compact relative density have been studied, while the particle sizes of Ti and B_4C and conditions of ball milling of the mixture (time and speed) were kept constant. A small particle size of B_4C relative to that of Ti has been chosen to enhance the contact and the solid-state reaction between them. This study was conducted by changing one factor at a time.

Finding the optimal processing parameters for producing sound magnesium matrix composites reinforced with a network of the *in-situ* formed TiC and TiB_2 particles is one of the main objectives of this work. Therefore, to reach this goal, composite samples were fabricated using AZ91D as a matrix metal at different processing parameters.

The results revealed that the processing parameters such as the processing temperature, holding time and green compact relative density play an important role in the *in-situ* reaction and hence in the fabrication of the composite.

Based on the results of studying the effect of the processing parameters on the fabrication of composites, it is recommended to fabricate the composites using a Ti–B_4C green compact of 70% *RD* at 900 °C for 1.5 h. A relatively uniform distribution of the reinforcing phases, TiC_x and TiB_2, forms as a network in the fabricated composites with very small amount of residual Ti, boron carbide and intermediate phases such as TiB, Ti_3B_4 and MgB_2 as shown in the microstructure and compositional mapping in Fig. 3 and the XRD patterns in Fig. 4. Moreover, the fabrication of the composites at these processing parameters avoids significant oxidation of Mg and formation of the ternary compound (Ti_2AlC) which can adversely affect the mechanical properties of the composites.

According to the compositional mapping, the observed overlap of the titanium, carbon and boron images proves the existence of the network of TiC and TiB_2 in the Mg matrix. It is worth noting that it is difficult to distinguish between the TiC and Ti borides phases because of the small difference in their mean atomic numbers making the discernment very difficult by SEM. On the other hand, Mg, boron carbide, and MgB_2 phases can be detected more easily due to the significant difference in their effective atomic numbers.

AZ91D matrix composites have also been fabricated using an MgH_2–(3Ti–B_4C) preform with 70% *RD* containing different weight percentages of MgH_2 powder at 900 °C for 1.5 h. Fig. 5 shows the microstructure and the compositional mapping of the composite fabricated using this 25 wt.% MgH_2–(3Ti–B_4C) preform. A reasonably uniform distribution of reinforcing phases, as a network of TiC_x and TiB_2 is observed without any residual intermediate phases. Furthermore, SEM observations reveal that no pores or microcracks are present in the microstructure of the as-fabricated TiC_x–TiB_2/AZ91D composites indicating that the composites are fully dense.

According to the compositional mapping of the composite sample fabricated at 1.5 h shown in Fig. 5, the observed overlap of the titanium, carbon and boron images indicates the existence of the network of TiC_x and TiB_2 in the Mg matrix. Furthermore, the compositional mapping reveals that Al is distributed not only inside the Mg matrix but also in the Mg-free regions indicating that the ternary compound (Ti_2AlC) is relatively uniformly distributed in the network of the reinforcing phases making its detection by SEM very difficult. However, the compositional mapping reveals the existence of Al in some concentrated areas.

To show the influence of adding MgH_2 powder to the 3Ti–B_4C preform on the volume fractions of Mg and the reinforcing phases, XRD analysis for both scenarios was carried out. The XRD results, summarized in Fig. 6, reveal that the volume percentage of magnesium in the fabricated composites increased after adding MgH_2 powder to the 3Ti–B_4C preform. However, more MgO was detected due to the decomposition of MgH_2 at low temperature forming Mg with high affinity to oxygen due, in part, to its high surface area. Also, the presence of Mg with high reactivity in the preform enhanced the reaction between Mg, Ti and B_4C and as a result, Mg composites were fabricated without any retained Ti, boron carbide or any intermediate phases such as TiB or MgB_2.

As shown in Fig. 7, the XRD spectra of the composite sample fabricated using 10 wt.% MgH_2–(3Ti–B_4C) preform reveals the formation of the TiC_x and TiB_2 reinforcing phases with very small residual intermediate phases such as TiB and MgB_2. On the other hand, the XRD patterns of the composite samples fabricated using 25 or 40 wt.% MgH_2 in the preform reveal the complete formation of the reinforcing phases without intermediate phases. However, the percentage of TiC_x in both cases is lower due to the formation of the ternary compound Ti_2AlC at the expense of TiC_x.

4.2. Reaction mechanism of the infiltrated Mg in the (Ti–B_4C) preform

4.2.1. The Ti–B_4C system

Based on the thermodynamic considerations discussed earlier, the solid-state reaction between Ti and B_4C to form TiC and TiB_2 is

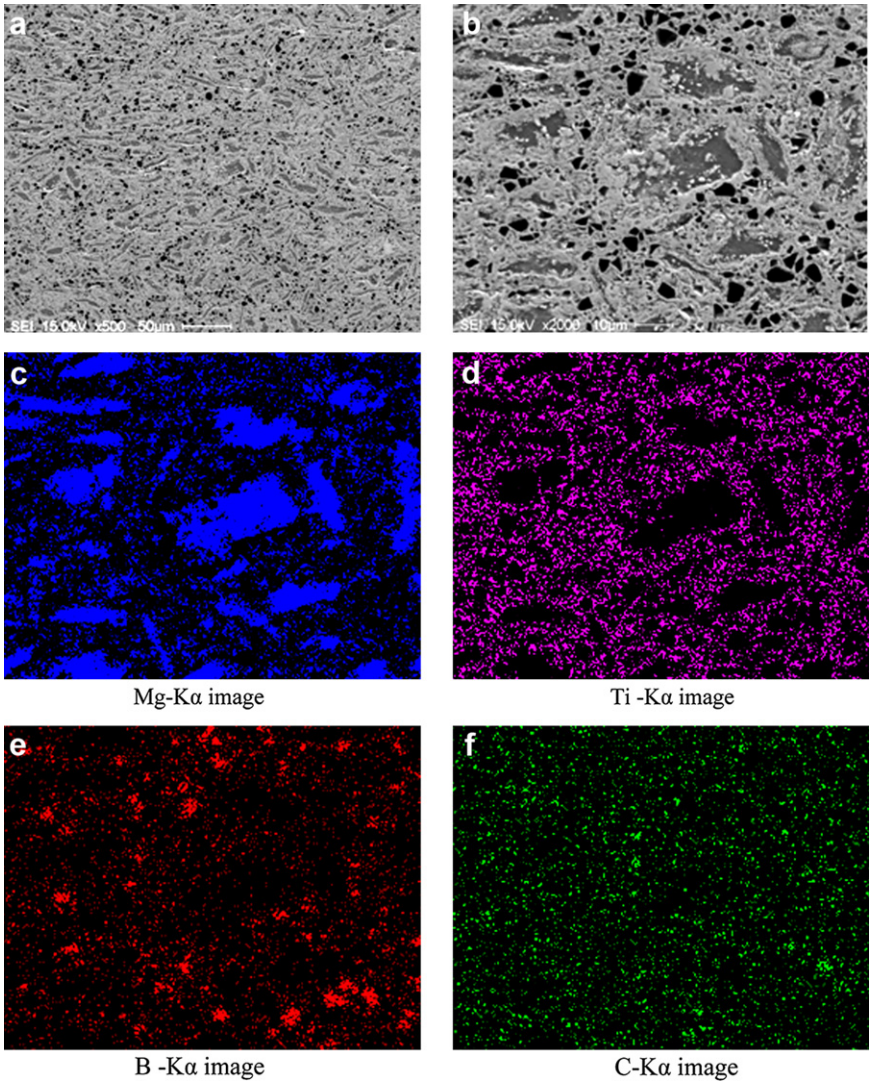

Fig. 3. SEM microstructure at (a) low magnification, (b) high magnification and X-ray compositional mapping of the TiC_x–TiB_2/AZ91D composites synthesized using a 3Ti–B_4C preform with 70% *RD* at 900 °C for 1.5 h (c) to (f) at high magnification (b).

the most favorable reaction but kinetically this reaction is very slow [10]. The XRD patterns of the two preforms heated to 900 °C for 1 h and 10 h compared with the starting powder mixture of 3Ti–B_4C are shown in Fig. 8.

The results reveal the formation of substoichiometric TiC_x prior to titanium borides with retained titanium and boron carbide ($B_{13}C_2$) after heat treatment for 1 h and 10 h. Also, it can be observed that TiB and Ti_3B_4 formed before TiB_2. At 1 h, the peaks' area of the TiB_2 phase is very small and increases with increasing the holding time to 10 h as shown in Fig. 8. There is still retained titanium and boron carbide indicating that the reaction is still incomplete even after 10 h holding time.

In the XRD analysis, the increase in the area under the peaks provides information about the kinetics of the reaction mechanism, as will be discussed below. It is also observed that the lattice constant of substoichiometric TiC_x increases with time due to the diffusion of C into TiC_x. As the stoichiometry (x) increases, the lattice parameter of TiC_x increases. Hence, based on the values of the lattice constant of TiC_x, the stoichiometry (x) in TiC_x at 10 h is consistent with that of $TiC_{0.67}$ according to Pearson's Handbook [11].

The results of the quenched (3Ti–B_4C) preform at different temperatures for 1 h holding time are shown in Fig. 9. No reaction took place at 600 °C where only Ti and B_4C peaks are observed, whereas, at 700 °C, Ti, boron carbide ($B_{13}C_2$) and TiC_x peaks are the main peaks in the XRD pattern. However, very low TiB and Ti_3B_4 peaks' intensities can also be observed. This shows that the substoichiometric TiC_x formed prior to titanium borides. At 800 °C, it was found that the area under the peaks of TiB, Ti_3B_4 and TiC_x increased while those of Ti and boron carbide decreased with very low TiB_2 peaks starting to appear. This shows that TiB and Ti_3B_4 phases formed prior to the TiB_2 phase.

Monitoring the change of area under the peaks of the phases reveals that the amounts of TiC_x and TiB_2 increased with increasing temperature to 900 °C while those of Ti, boron carbide, TiB and Ti_3B_4 decreased and it can be said that the retained Ti is very small and can be neglected at 900 °C. These results indicate that the reaction is still incomplete even at 900 °C for 1 h.

The variations of the lattice parameters of Ti and B_4C formed after heat treatment of 3Ti–B_4C samples at different temperatures after 1 h holding time are presented in Table 1. It can be observed that the lattice parameters of Ti increase with increasing temperature till 700 °C. This means that C-saturated Ti, $Ti_{C\text{-}sat.}$ formed prior to titanium carbide due to the diffusion of C from B_4C into Ti. With increasing temperature, the substoichiometric TiC_x forms while the lattice parameters of the retained Ti decreased again. However, the

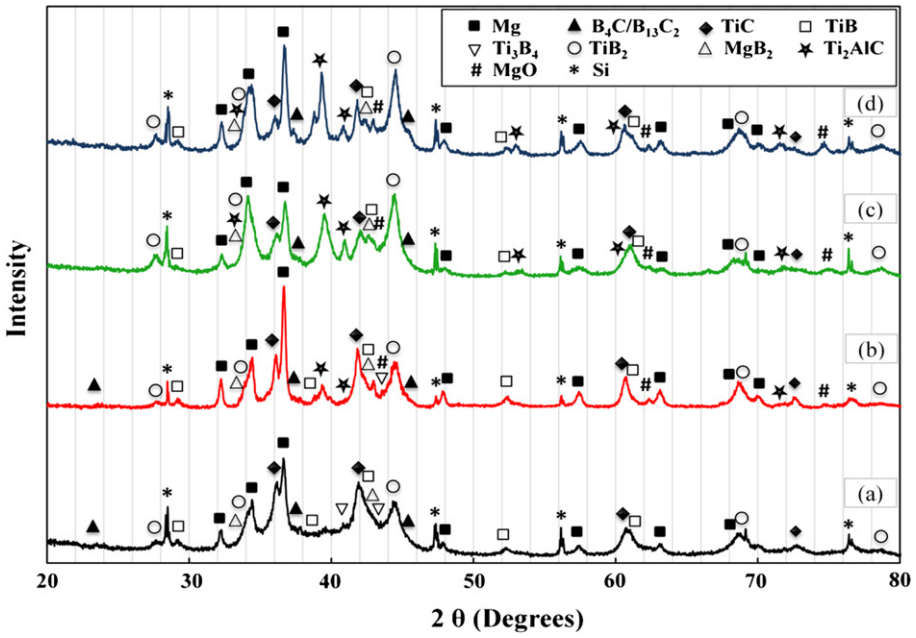

Fig. 4. XRD pattern of the AZ91D alloy MMCs fabricated using a 3Ti−B_4C preform with 70% *RD* at 900 °C for different holding times: (a) 1 h, (b) 1.5 h, (c) 3 h, and (c) 6 h.

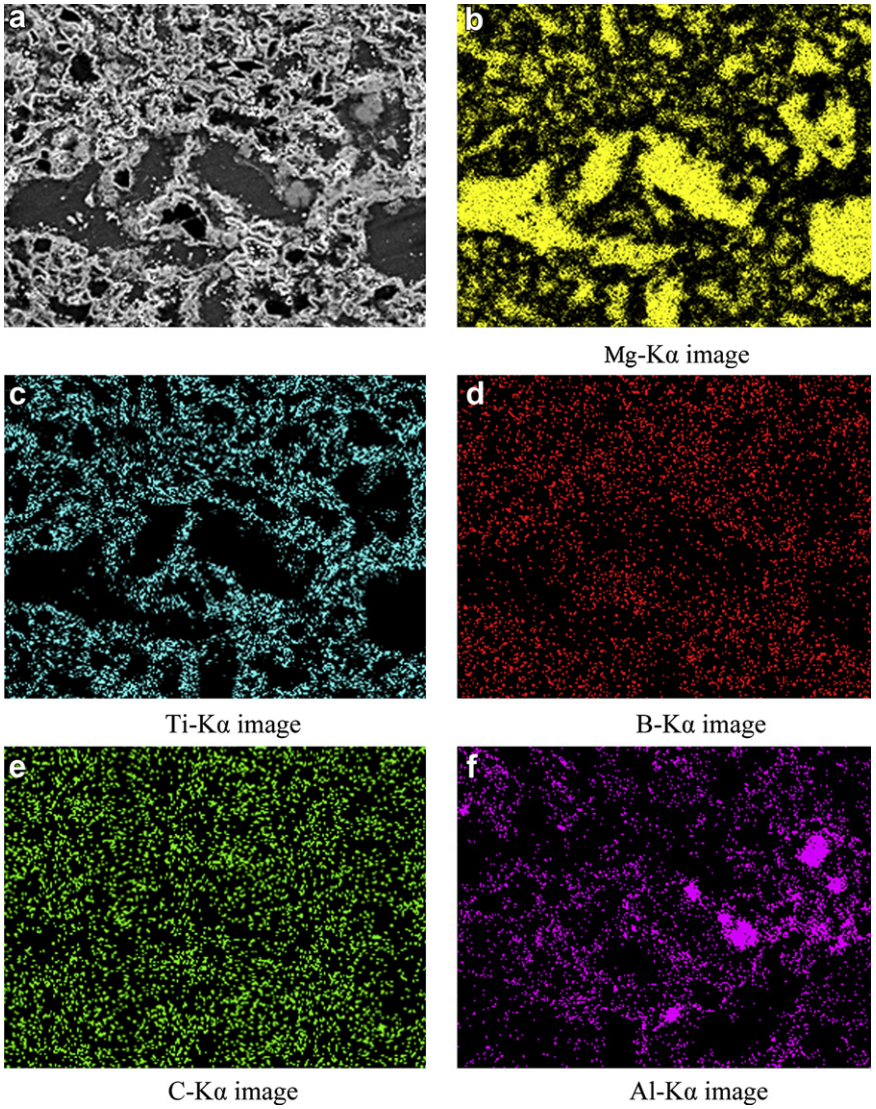

Fig. 5. SEM microstructure (a) and X-ray compositional mapping of the TiC_x−TiB_2/AZ91D composites synthesized at 900 °C for 1.5 h using a 25 wt.% MgH_2−(3Ti−B_4C) preform with 70% *RD* (b) to (f).

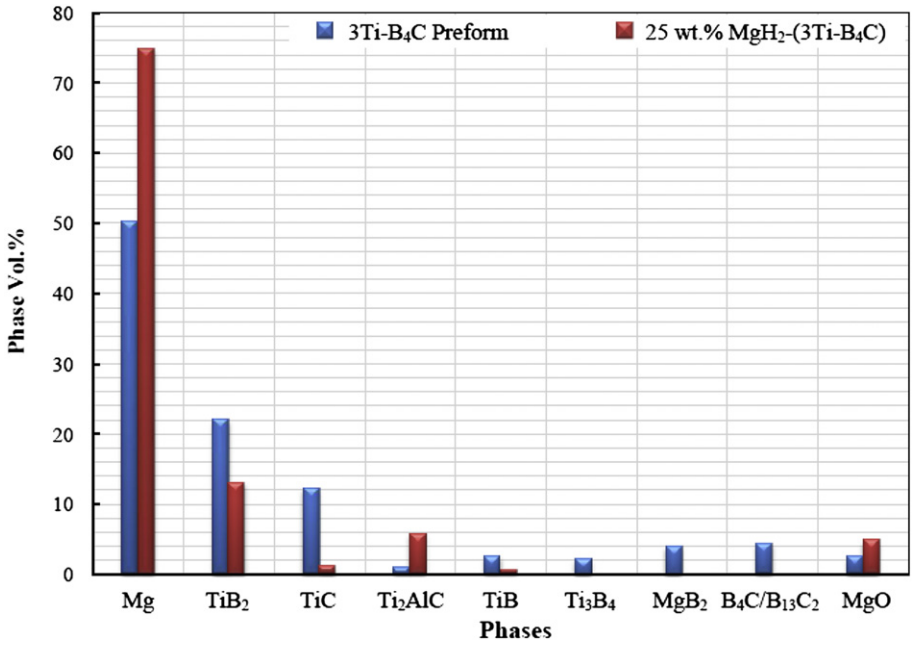

Fig. 6. Phase volume percentage of the AZ91D alloy MMCs fabricated at 900 °C for 1.5 h using different preforms (a) 3Ti–B_4C and (b) 25 wt.% MgH_2–(3Ti–B_4C) preforms with 70 % *RD*.

amount of the C-saturated Ti is very small and can be neglected after 700 °C. The range of the lattice parameters of the boron carbide is found to be consistent with that of the standard lattice constants of $B_{13}C_2$ reported in Pearson's Handbook [11].

Thus, based on these results and the crystallographic data of the various phases in the system, the reaction sequence of the Ti–B_4C system can be presented as follows:

$$3Ti + B_4C = Ti_{C-sat.} + B_{13}C_2 \rightarrow Ti_{C-sat.} + B_{13}C_2 + TiC_x \quad (10)$$

$$\rightarrow Ti + B_{13}C_2 = TiC_x + TiB \quad (11)$$

$$\rightarrow Ti + B_{13}C_2 + TiC_x + TiB + Ti_3B_4 \quad (12)$$

$$\rightarrow B_{13}C_2 = TiC_x + TiB + Ti_3B_4 + TiB_2 \rightarrow TiC_x + TiB_2 \quad (13)$$

However, the complete formation of TiC_x and TiB_2 requires a very long time if the 3Ti–B_4C preform is heat-treated according to the same heating cycle used for the fabrication of the composite (Fig. 2(b)). This reaction sequence is based on different partial reactions that involve Ti and B_4C and/or the intermediate phases as follows:

$$5/6Ti + 1/6B_4C = 2/3TiB + 1/6TiC \quad (14)$$

$$16/17TiB + 1/17B_4C = 5/17Ti_3B_4 + 1/17TiC \quad (15)$$

$$3/4Ti_3B_4 + 1/4B_4C = 2TiB_2 + 1/4TiC \quad (16)$$

Zhao and Cheng [12] suggested that these reactions take place at relatively low temperatures ($T \leq 1300$ °C) when they investigated the formation of TiC–TiB_2 composites by reactive sintering of

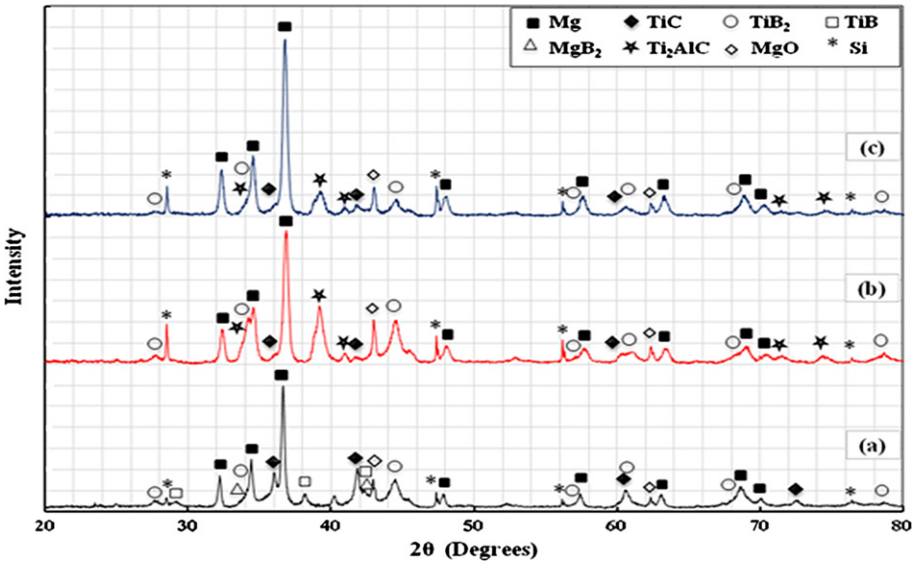

Fig. 7. XRD pattern of the AZ91D alloy MMCs fabricated at 900 °C for 1.5 h using MgH_2–(3Ti–B_4C) preforms with different MgH_2 weight percentages (a) 10, (b) 25 and (c) 40 wt.%.

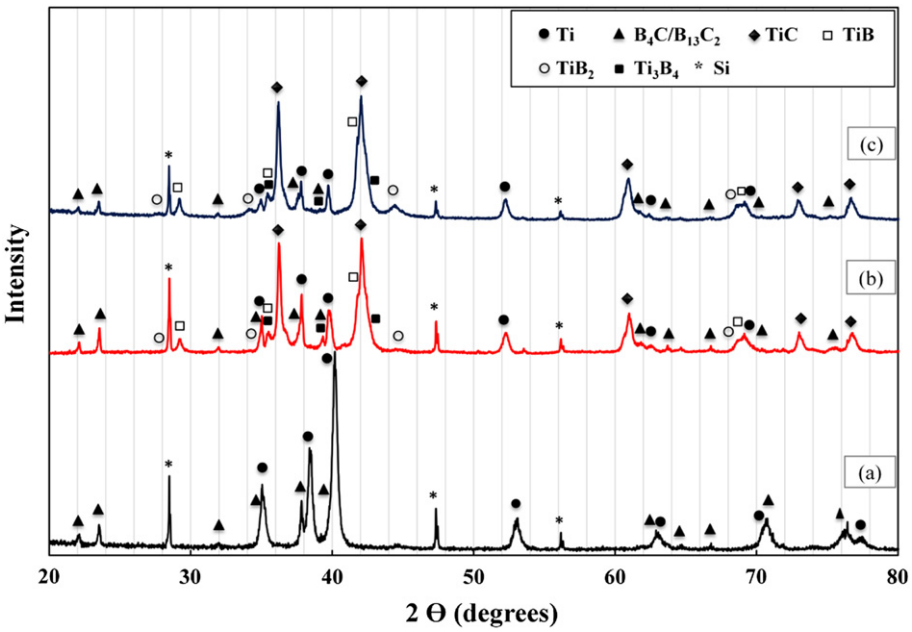

Fig. 8. XRD pattern of (a) the starting 3Ti–B_4C powder mixture and 3Ti–B_4C preforms: (b) after heat treatment at 900 °C for 1 h and (c) after heat treatment at 900 °C for 10 h.

3Ti–B_4C compacts at temperatures between 950 and 1650 °C. The formation of substoichiometric TiC_x prior to the titanium borides was also proposed by Zhao and Cheng [12]. This is attributed to the fact that the diffusivity of carbon in Ti is much greater than that of boron [13]. Despite the strong covalent bonds between the atoms in the boron carbide structure, carbon diffuses away from boron carbide faster than boron. Therefore, due to the reaction of Ti and B_4C, TiC_x phase forms prior to titanium borides leaving a B-rich boron carbide core in the center of the particles as Shen et al. [13] observed.

The conversion of B_4C to $B_{13}C_2$ is consistent with Emin's suggestion [14]. According to this suggestion, with decreasing carbon concentration in B_4C, boron substitutes for carbon in the intericosahedral chains converting the C–B–C chains to C–B–B chains (i.e., B_4C changes to $B_{13}C_2$). This also agrees with the work of Shen et al. [13].

4.2.2. The Mg–B_4C system

It appears that without magnesium, the solid-state reaction between Ti and B_4C to form TiC_x and TiB_2 is kinetically very slow during the heating cycle used for the fabrication of the composites especially in the temperature range used here. At 800 °C and below, it was found that no spontaneous infiltration could be attained without adding wetting agent such as Ti to the B_4C powder. Fig. 10 shows the XRD patterns of heat-treated B_4C and after infiltration of molten Mg to B_4C preform at 900 °C for 1 h.

However, the results at 900 °C revealed that magnesium infiltrated the preform and the main diffraction peaks corresponding to

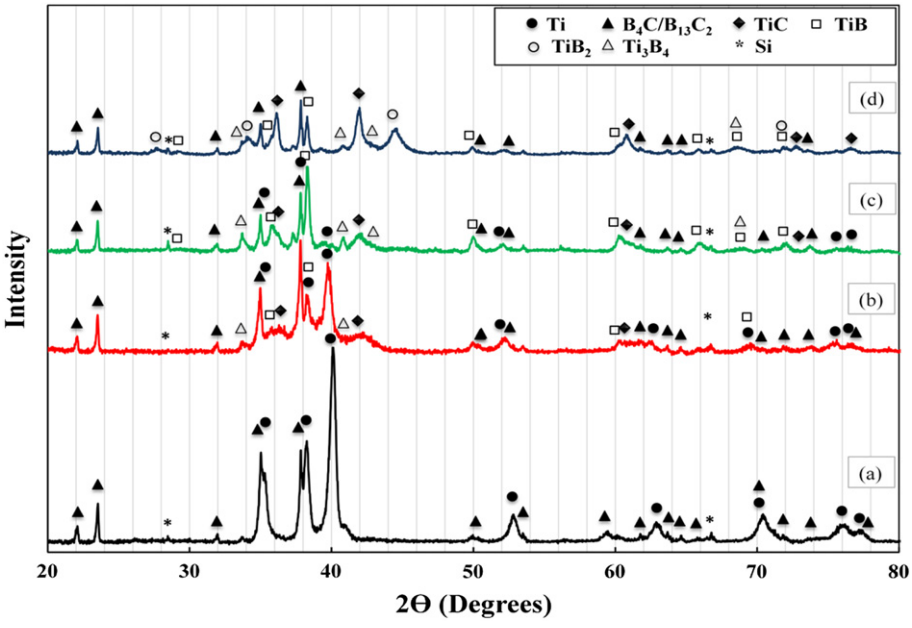

Fig. 9. XRD patterns of heat-treated 3Ti–B_4C samples quenched from different temperatures: (a) 600 °C, (b) 700 °C, (c) 800 °C, and (d) 900 °C after 1 h holding time.

Table 1
Lattice parameters of Ti and boron carbide for heat-treated 3Ti–B_4C compact samples at different temperatures for 1 h holding time.

Sample	Temp.	Ti		Boron carbide	
		a (Å)	*c* (Å)	*a* (Å)	*c* (Å)
3Ti–B_4C	600 °C	2.9565	4.7108	5.6029	12.0934
	700 °C	2.9767	4.7786	5.6074	12.1045
	800 °C	2.9504	4.6953	5.6047	12.0884
	900 °C	2.900	4.7030	5.6039	12.09

Mg and MgB_2 were detected but at the same time, there are MgB_4 and retained boron carbide (B_4C) phases in the sample as shown in the figure. This means that magnesium wets B_4C at 900 °C through an interfacial reaction even without adding wetting agent as Ti. This is because the surface tension of liquid decreases with increasing temperature and this agrees with the results of Palmer [15].

Fig. 11 shows the XRD spectra of quenched Mg–B_4C samples at different temperatures for 1 h. The results revealed that after heat treatment at 600 °C, the principal peaks are those of Mg and B_4C. However, very small MgO particles have formed due to the partial reaction of Mg with oxygen. At 700 °C, the peaks of MgB_2, MgB_4 and MgC_2 appeared beside those of Mg and retained B_4C. MgC_2 formed due to the reaction of the liberated carbon with Mg in the system but this phase is unstable and rapidly decomposes. With increasing temperature, the area under the peaks of MgB_2 increased while those of Mg and retained B_4C decreased till those of Mg disappeared at 900 °C.

It is worth noting that despite the fact that the molar ratio of Mg to B_4C is higher than that required to complete the reaction between Mg and B_4C to form MgB_2, it was found that Mg disappeared while there was still retained B_4C in the system. The reason is the partial reaction of Mg with oxygen as mentioned earlier.

Based on the XRD results, it can be suggested that molten magnesium reacts with B_4C to form magnesium diboride liberating elemental carbon. This reaction is an exothermic reaction providing heat for further reaction to occur in the system. Hence, the reaction mechanism is as follows:

$$2Mg + B_4C = 2MgB_2 + C \quad (17)$$

This result agrees with what is suggested by Kevorkijan and Skapin [16]. Also, the presence of MgB_4 peaks in the XRD pattern proves that MgB_2 partially decomposes forming MgB_4 and Mg gas that diffuses through the thin film of MgB_4 as follows:

$$MgB_2 = \frac{1}{2}MgB_4 + \frac{1}{2}Mg(g) \quad (18)$$

This agrees with the results obtained by Brutti et al. [17].

4.2.3. Infiltrating Mg in the (Ti–B_4C) preform

Fig. 12 shows the XRD patterns of the 3Ti–B_4C preform (no Mg) compacted at 70% *RD* after heat treatment at 900 °C for 1 h in relation to the Mg matrix composite sample fabricated at the same temperature and holding time using a 3Ti–B_4C preform of the same relative density.

It can be observed that substoichiometric TiC_x formed in both cases while significant amounts of TiB_2 formed after infiltration of Mg even at this short time. This reveals the role of infiltrated molten Mg or Mg alloy in the reaction which was very important especially because no other metal powder, such as Al, was added to the Ti–B_4C system.

Based on the reaction sequences of the individual systems, Ti–B_4C and Mg–B_4C, the reaction mechanism of the complete infiltrated Mg–(Ti–B_4C) system after the infiltration of molten Mg alloy through the 3Ti–B_4C preform can be presented as follows:

$$3Ti + B_4C + Mg = Ti + B_{13}C_2 + TiC_x + TiB + MgB_2 \quad (19)$$

TiC_x formed due to the reaction between Ti and B_4C (Eq. 10) and also the diffusion of atomic C liberated by the reaction between Mg and B_4C (Eq. 17) into Ti according to the following equation:

$$Ti + C = TiC_x \quad (20)$$

MgB_2 partially decomposes forming MgB_4 and Mg gas that diffuses through the thin film of MgB_4 according to Eq. 18. On the

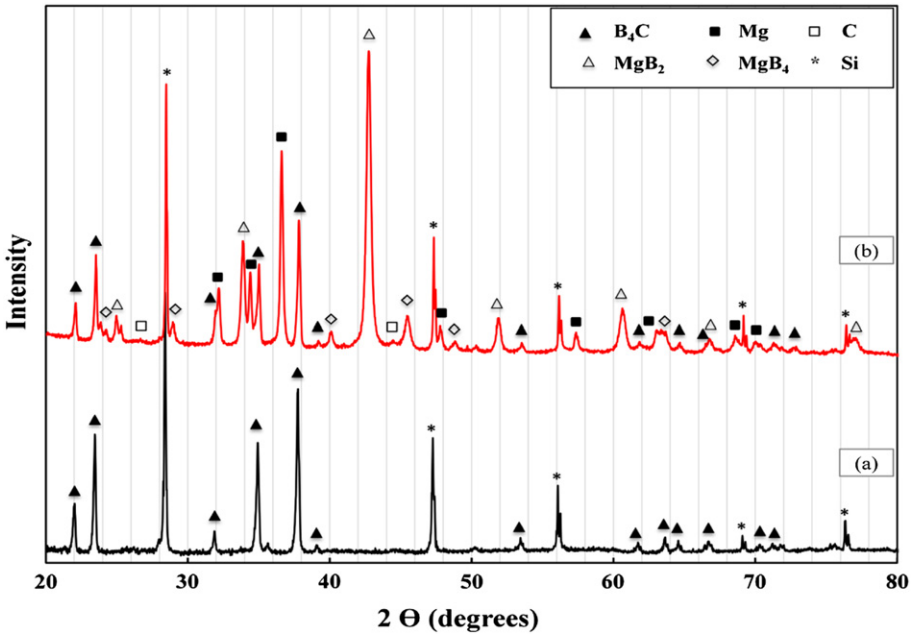

Fig. 10. XRD pattern of (a) heat-treated B_4C preform and (b) after infiltration of molten Mg into B_4C preform at 900 °C for 1 h.

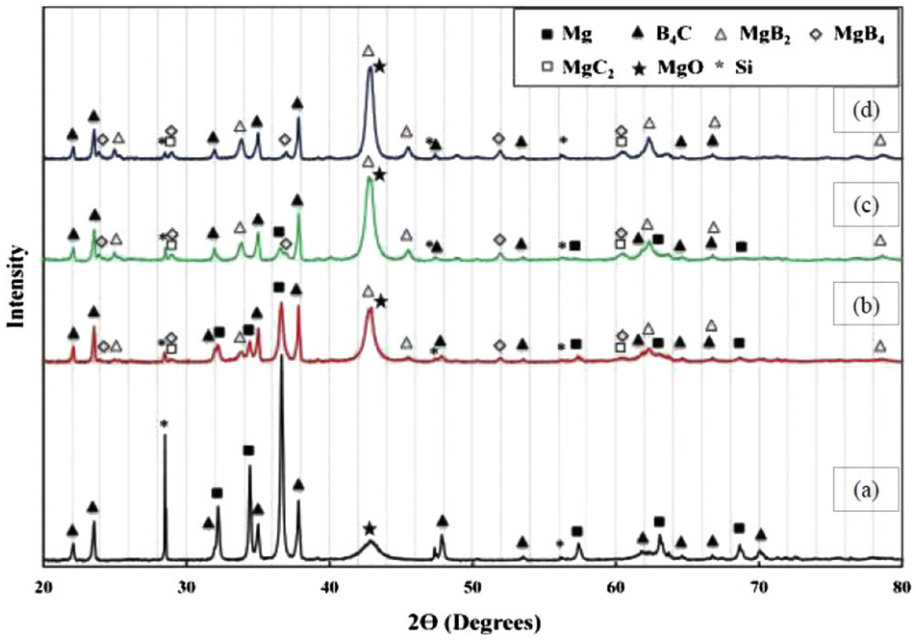

Fig. 11. XRD patterns of heat-treated Mg–B_4C samples quenched from different temperatures (a) 600, (b) 700, (c) 800 and (d) 900 °C after 1 h holding time.

other hand, TiB reacts with B_4C forming Ti_3B_4 and TiC according to Eq. 15 then:

$$3Ti + B_4C + Mg = Ti + B_{13}C_2 + TiC_x + TiB + Ti_3B_4 + MgB_2 + MgB_4 \quad (21)$$

Considering that:

$$Ti + \frac{1}{2}MgB_4 = 2TiB_2 + \frac{3}{2}Mg \quad (22)$$

Reaction 21 leads to:

$$B_{13}C_2 + TiC_x + TiB + Ti_3B_4 + TiB_2 + MgB_2 \quad (23)$$

Since MgB_2 reacts with TiB forming TiB_2 and titanium borides, TiB and Ti_3B_4, react with the retained boron carbide as presented earlier in the reaction mechanism of the Ti–B_4C system, the reaction between Ti, B_4C and infiltrated molten Mg alloy is finally obtained as follows:

$$3Ti + B_4C + Mg = TiC_x + 2TiB_2 + Mg \quad (24)$$

Based on these observations, it can be concluded that Mg not only infiltrates through the 3Ti–B_4C preform and thus densifies the fabricated composite as a matrix metal but also acts as an intermediary that makes the reaction possible at a lower temperature than that required for solid-state reaction between Ti and B_4C.

Finally, the study of the *in-situ* reaction mechanism is very important to understand and interpret the microstructure of the produced composites and their properties. The infiltration of Mg melt through the preform of (3Ti–B_4C) basically depends on its viscosity and the wettability between Ti, B_4C and/or the *in-situ* formed TiC. Mg infiltrated the preform through the pores by the capillary force resulting in dense microstructure of magnesium matrix composites.

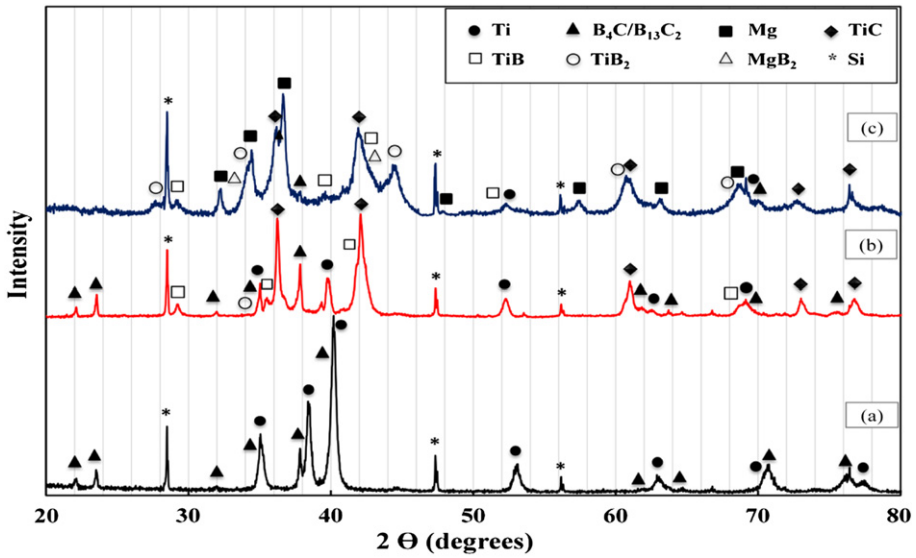

Fig. 12. XRD pattern of (a) the starting 3Ti–B_4C powder mixture, (b) heat-treated 3Ti–B_4C preform at 900 °C for 1 h and (c) Mg composite fabricated at 900 °C for 1 h.

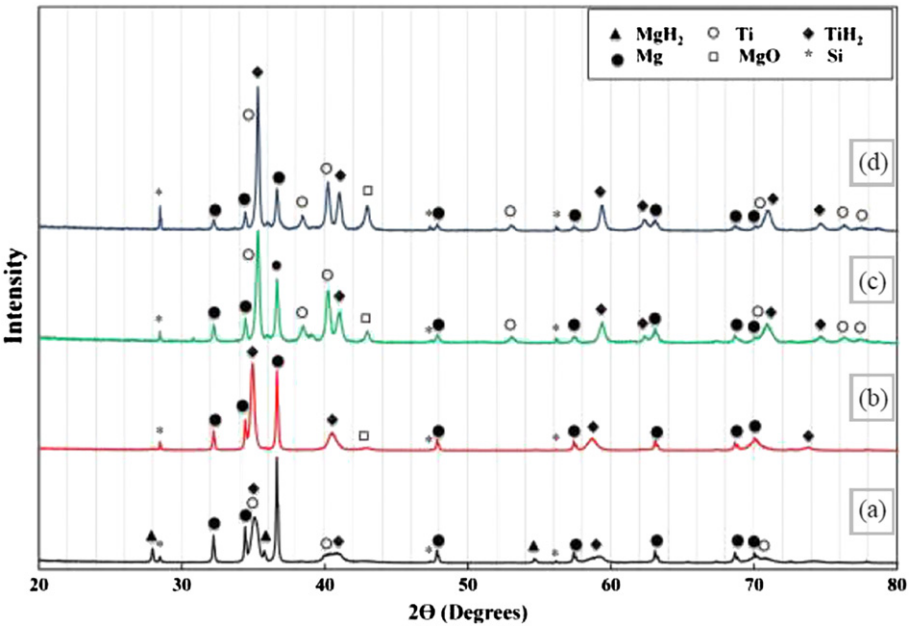

Fig. 13. XRD patterns of heat-treated MgH_2–Ti samples quenched from different temperatures (a) 400, (b) 600, (c) 700 and (d) 800 °C after 1 h holding time.

4.3. Reaction mechanism of the infiltrated Mg in the (MgH_2–Ti–B_4C) preform

4.3.1. The MgH_2–Ti system

The XRD patterns of heat-treated MgH_2–Ti compacts at different temperatures from 400 to 800 °C for 1 h followed by quenching in water are shown in Fig. 13.

The results reveal that at 400 °C, Mg, MgH_2, Ti and TiH_2 are present in the sample. However, the only main peaks at 600 °C are those of Mg and TiH_2 while with increasing temperature, Ti appeared again along with Mg and TiH_2 at 700 and 800 °C. The change in the lattice constant of TiH_2 as shown in Table 2 reveals that the highest value is for 600 °C which decreases with increasing temperature. Based on this, TiH_2 that formed at the beginning has a high content of hydrogen stemming from the decomposition of MgH_2. With increasing temperature, the rate of hydrogen release increased due to the decomposition of TiH_2.

Also, the XRD patterns of the MgH_2–Ti preform and the sample after infiltration of the molten AZ91D alloy into this preform heated to 900 °C for 1.5 h are shown in Fig. 14.

Based on the XRD results, it can be observed that MgH_2 decomposed at low temperature (around 400 °C) forming Mg and releasing hydrogen according to the following equation:

$$MgH_2 \rightarrow Mg + H_2 \quad (25)$$

Then Ti reacts with H_2 to form TiH_2 which decomposes with increasing temperature forming more reactive Ti due to an increase in its surface area and releasing hydrogen as follows:

$$Ti + H_2 \xrightarrow{\sim 600^{\circ}C} TiH_2 \quad (26)$$

$$TiH_2 \xrightarrow{\sim 700^{\circ}C} Ti + H_2 \quad (27)$$

Table 2
Lattice parameters of TiH_2 for heat-treated MgH_2–Ti samples at different temperatures.

Sample	Processing parameters	Lattice constant of TiH_2, a, (Å)
MgH_2–Ti	400 °C/1 h	4.4306
	600 °C/1 h	4.453886
	700 °C/1 h	4.405647
	800 °C/1 h	4.404136

4.3.2. The MgH_2–B_4C system

The XRD patterns of the MgH_2–B_4C preform with 70% *RD* and the sample after infiltration with molten AZ91D alloy processed at 900 °C for 1.5 h are shown in Fig. 15. Based on the XRD results, it is found that the reaction mechanism of the MgH_2–B_4C system is similar to that of the Mg–B_4C system. The difference between the two cases is that Mg formed by the decomposition of MgH_2 is more chemically reactive due to its higher surface area than Mg in the Mg–B_4C system. By comparing the MgH_2–B_4C with the Mg–B_4C system, it is found that the magnesium formed by the decomposition of MgH_2 is more reactive than Mg powder in the Mg–B_4C system. This can be proved by its high affinity for oxygen and forming MgO as shown in Fig. 15.

During and after complete infiltration of liquid magnesium through the MgH_2–B_4C preform, some of the molten magnesium reacts with some of the remaining boron carbide, as mentioned earlier during the discussion of the reaction mechanism of the Mg–Ti–B_4C system, while the remaining molten magnesium just fills the pores in the preform.

4.3.3. Infiltrating Mg in the (MgH_2–Ti–B_4C) preform

Fig. 16 shows the XRD spectra of the 25 wt.% MgH_2–(3Ti–B_4C) preform mixture, that was compacted at 70% *RD* and heat-treated at 900 °C for 1.5 h, and an AZ91D matrix composite sample fabricated at the same temperature and holding time using the same preform.

It can be observed that substoichiometric TiC_x formed in both cases while TiB_2 formed significantly after infiltration of molten magnesium through the preform. The peaks of the formed TiB_2 before Mg infiltration are very small. Also, there are still peaks of retained Ti and boron carbide and those of the intermediate phases MgB_2 and TiB in the case of the heat-treated preform before infiltration of molten AZ91D alloy. This proves that the reaction is

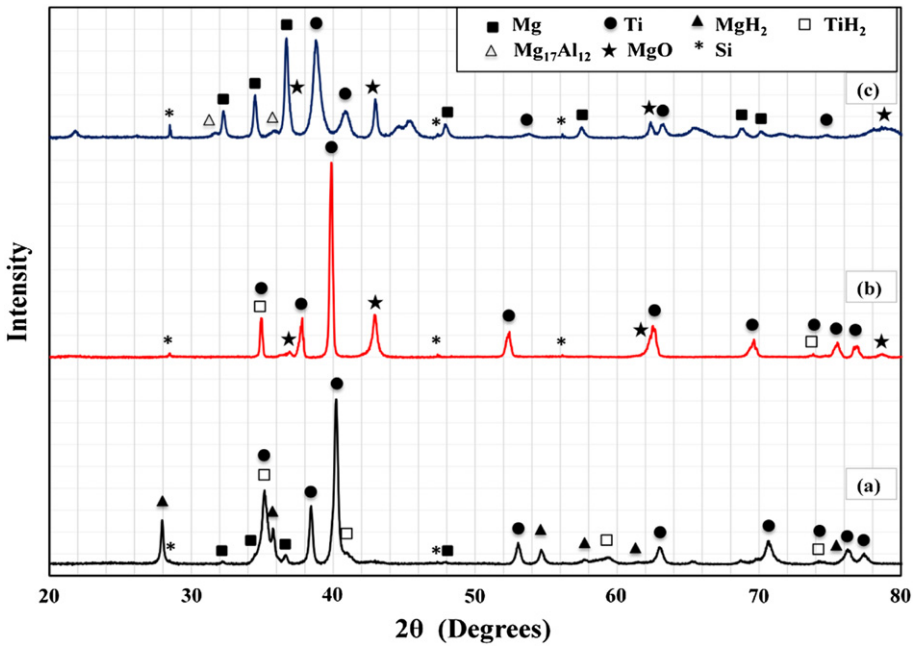

Fig. 14. XRD pattern of (a) MgH_2–Ti mixture (b) heat-treated MgH_2–Ti preform and (c) after infiltration of molten AZ91D into this preform at 900 °C for 1.5 h.

incomplete. The complete reaction after infiltration of molten magnesium without retained Ti and boron carbide and intermediate phases reveals the role of MgH_2 in this reaction mechanism. The MgH_2 plays a similar role as the infiltrated magnesium before and during the infiltration process.

Based on these results, the *in-situ* reaction mechanism of the infiltrated Mg–(MgH_2–Ti–B_4C) system was investigated based on the reaction mechanism of MgH_2–Ti–B_4C and that of the infiltrated Mg–(3Ti–B_4C) which was discussed earlier.

It was found that the reaction mechanism of the whole infiltrated Mg–(MgH_2–Ti–B_4C) system is similar to that of the infiltrated Mg–(Ti–B_4C) system. The difference between the two cases is that the Mg that formed by the decomposition of MgH_2 is more chemically reactive due to its higher surface area than Mg in the Mg–Ti–B_4C system. Also, Ti that formed after the decomposition of TiH_2 is more chemically reactive due to its higher surface area than Ti in the Mg–Ti–B_4C system making the reaction between Ti and B_4C much faster and the same applies for the case of Mg with B_4C.

Also, it is observed that the ternary Ti_2AlC compound formed when AZ91D is used. Ti_2AlC forms by the diffusion of Al into substoichiometric TiC_x at high temperature. The amount of Ti_2AlC is higher if compared with that formed without MgH_2 in the preform. The reason behind this is that the reaction is faster by the presence of MgH_2 in the preform and then the formation of

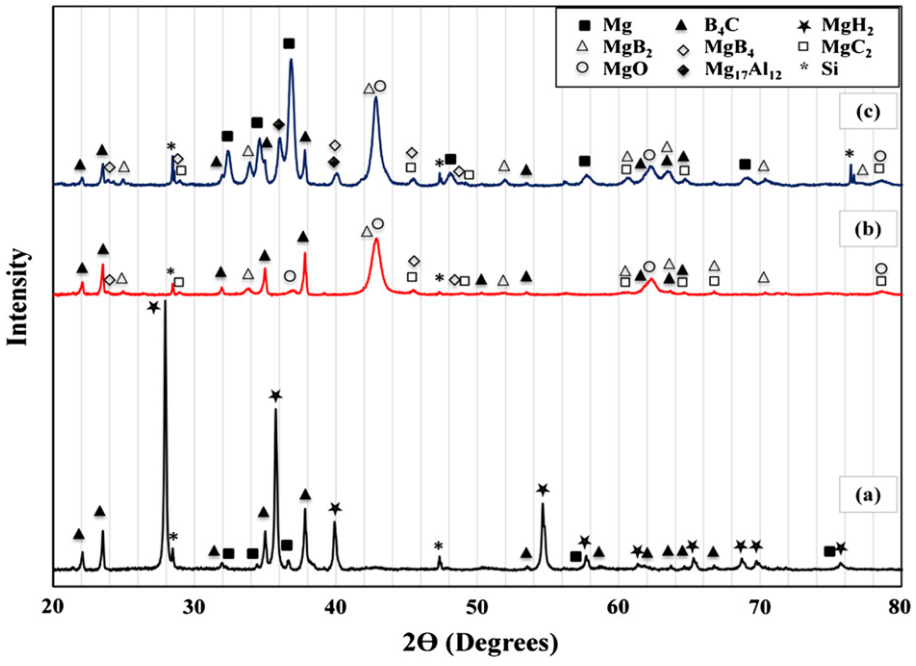

Fig. 15. XRD pattern of samples (a) MgH_2–B_4C mixture, (b) heat-treated MgH_2–B_4C preform and (c) after infiltration of molten AZ91D into this preform at 900 °C for 1.5 h.

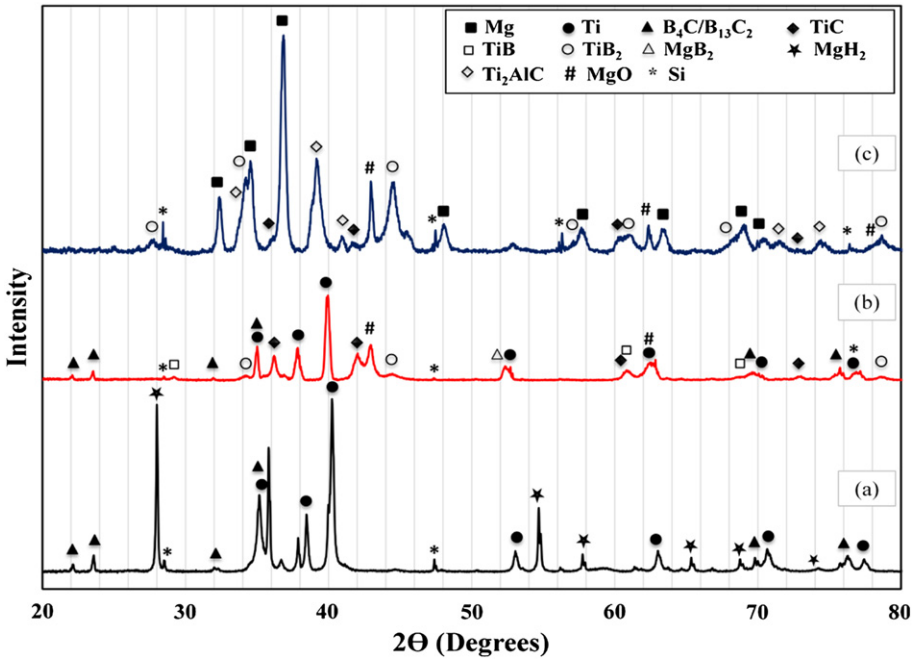

Fig. 16. XRD pattern of samples (a) 25 wt.% MgH_2–(3Ti–B_4C) mixture, (b) heat-treated 25 wt.% MgH_2–(3Ti–B_4C) preform and (c) after infiltration of molten AZ91D into this preform at 900 °C for 1.5 h.

substoichiometric TiC_x is very fast allowing more formation of this ternary compound compared with the case without MgH_2 in the preform within the same holding time. It can be concluded that MgH_2 after decomposition plays the role of magnesium to react with B_4C before and during the infiltration of molten magnesium or magnesium alloy into the preform.

5. Conclusions

(1) AZ91D magnesium matrix composites reinforced with a network of TiC_x and TiB_2 particles were successfully synthesized using a practical and low cost *in-situ* reactive infiltration technique.
(2) The microstructure of TiC_x–TiB_2/AZ91D composites is essentially evolved from the reaction between Ti, B_4C and the Mg melt. The substoichiometric TiC_x forms prior to TiB_2 because the diffusion of carbon in Ti is much faster than that of boron.
(3) Studying the *in-situ* reaction mechanism revealed the role of the Mg melt in the system where it not only infiltrates through the 3Ti–B_4C preform and thus densifies the fabricated composites as a matrix metal but also acts as an intermediary that makes the reaction possible at a lower temperature than that required in the case of the solid-state reaction between Ti and B_4C.
(4) The addition of MgH_2 powder to the 3Ti–B_4C preform significantly accelerates the reaction between Ti and B_4C and raises the Mg content in the fabricated composites.

Acknowledgements

The authors thank Egyptian ministry of defense for giving the first author the opportunity to accomplish this work at Concordia University and for financial support from NSERC. The authors also wish to thank Research Associate, Dr. Dmytro Kenorkov, for his valuable help in some experimental work.

References

[1] Q.F. Guan, H.Y. Wang, X.L. Li, Q.C. Jiang, Effect of compact density on the fabrication of Mg–TiC composites, Journal of Materials Science Vol. 39 (No. 16) (2004) 5569–5572.
[2] Q.C. Jiang, X.L. Li, H.Y. Wang, Fabrication of TiC particulate reinforced magnesium matrix composites, Scripta Materialia Vol. 48 (No. 6) (2003) 713–717.
[3] B.L. Mordike, T. Ebert, Magnesium: properties–applications–potential, Materials Science and Engineering A Vol. 302 (No. 1) (2001) 37–45.
[4] Y. Wang, H.Y. Wang, K. Xiu, H.Y. Wang, Q.C. Jiang, Fabrication of TiB_2 particulate reinforced magnesium matrix composites by two-step processing method, Materials Letters Vol. 60 (No. 12) (2006) 1533–1537.
[5] S.C. Tjong, Z.Y. Ma, Microstructural and mechanical characteristics of in situ metal matrix composites, Materials Science and Engineering: R: Reports Vol. 29 (No. (3–4)) (2000) 49–113.
[6] L.Q. Chen, Q. Dong, M.J. Zhao, J. Bi, N. Kanetake, Synthesis of TiC/Mg composites with interpenetrating networks by *in-situ* reactive infiltration process, Materials Science and Engineering: A Vol. 408 (No. (1–2)) (2005) 125–130.
[7] B. Ma, H. Wang, Y. Wang, Q. Jiang, Fabrication of $(TiB_2–TiC)_p$/AZ91 magnesium matrix hybrid composite, Journal of Materials Science Vol. 40 (No. 17) (2005) 4501–4504.
[8] X. Zhang, H. Wang, L. Liao, X. Teng, N. Ma, The mechanical properties of magnesium matrix composites reinforced with (TiB_2+TiC) ceramic particulates, Materials Letters Vol. 59 (No. 17) (2005) 2105–2109.
[9] Q. Dong, L.Q. Chen, M.J. Zhao, J. Bi, Synthesis of TiC_p reinforced magnesium matrix composites by *in-situ* reactive infiltration process, Materials Letters Vol. 58 (No. 6) (2004) 920–926.
[10] T. Hitoshi, A. Taroh, O. Tadashi, K. Koji, Synthesis of TiB_2–TiC Composites by solid-state reaction between B_4C and Ti Powders, Journal of the Ceramic Society of Japan Vol. 107 (No. 11) (1999) 1041–1045.
[11] H. Putz, and K. Brandenburg: Pearson's crystal data, crystal structure database for inorganic compounds, CD-ROM software version 1.3.
[12] H. Zhao, Y.B. Cheng, Formation of TiB_2–TiC composites by reactive sintering, Ceramics International Vol. 25 (No. 4) (1999) 353–358.
[13] P. Shen, B. Zou, S. Jin, Q. Jiang, Reaction mechanism in self-propagating high temperature synthesis of TiC–TiB_2/Al composites from an Al–Ti–B_4C system, Materials Science and Engineering: A Vol. 454–455 (2007) 300–309.
[14] D. Emin, Structure and single-phase regime of boron carbides, Journal of Review Letters B Vol. 38 (1988) 6041–6055.
[15] S.J. Palmer, The effect of temperature on surface tension, Journal of Physics Education Vol. 11 (No. 2) (1976) 119–120.
[16] V. Kevorkijan, S.D. Skapin, Mg–B_4C composites with a high volume fraction of fine ceramic reinforcement, Journal of Materials and Manufacturing Processes Vol. 24 (2009) 1337–1340.
[17] S. Brutti, G. Balducci, G. Gigli, A. Ciccioli, P. Manfrinetti, A. Palenzona, Thermodynamic and kinetic aspects of decomposition of MgB_2 in vacuum: implications for optimization of synthesis conditions, Journal of Crystal Growth Vol. 289 (No.2) (2006) 578–586.